The *shh* limb enhancer is activated in patterned limb regeneration but not in hypomorphic limb regeneration in *Xenopus laevis*

Reimi Tada[1,*], Takuya Higashidate[2,*], Takanori Amano[3], Shoma Ishikawa[1], Chifuyu Yokoyama[1], Saki Nara[1], Koshiro Ishida[1], Akane Kawaguchi[4,#], Haruki Ochi[5], Hajime Ogino[6], Nayuta Yakushiji-Kaminatsui[7], Joe Sakamoto[8], Yasuhiro Kamei[8,9], Koji Tamura[2], and Hitoshi Yokoyama[1‡].

Affiliation: [1]Department of Biochemistry and Molecular Biology
Faculty of Agriculture and Life Science, Hirosaki University
3 Bunkyo-cho, Hirosaki, Aomori 036-8561, Japan.
[2]Department of Ecological Developmental Adaptability Life Sciences,
Graduate School of Life Sciences, Tohoku University,
Aramaki-Aza-Aoba 6-3, Aoba-ku, Sendai 980-8578, Japan.
[3]Next Generation Human Disease Model Team
RIKEN BioResource Research Center
3-1-1 Koyadai, Tsukuba, Ibaraki, 305-0074, Japan
[4]Graduate School of Biological Sciences, Nara Institute of Science and Technology (NAIST), Ikoma, Nara, Japan.
[5]Institute for Promotion of Medical Science Research, Faculty of Medicine, Yamagata University, Yamagata 990-9585, Japan.
[6]Amphibian Research Center / Graduate School of Integrated Sciences for Life, Hiroshima University, 1-3-1 Kagami-yama, Higashi-Hiroshima, Hiroshima 739-8526, Japan.
[7]RIKEN Center for Integrative Medical Sciences (IMS)
1-7-22 Suehiro-cho, Tsurumi-ku, Yokohama 230-0045, Japan
[8] Laboratory for Biothermology, National Institute for Basic Biology, Myodaiji, Okazaki, Aichi 444-8585, Japan
[9]Department of Basic Biology in the School of Life Science of the Graduate University for Advanced Studies (SOKENDAI), Okazaki,

Aichi 444-8585, Japan
[#]Present address: Molecular Life History Laboratory, Department of Genomics and Evolutionary Biology, National Institute of Genetics, Japan
*These authors contributed equally to this work.

Running Title: *shh* enhancer in limb regeneration

Key words: limb regeneration; *shh*; long-range enhancer; *Xenopus*; regenerative capacity

Summary statement: We visualized the activity of a limb-specific enhancer of *shh* in the regenerating limb of an amphibian, *Xenopus*: it correlates with the capacity for regeneration of a well-patterned limb.

[‡]Author for correspondence:
Hitoshi Yokoyama
Department of Biochemistry and Molecular Biology
Faculty of Agriculture and Life Science, Hirosaki University
3 Bunkyo-cho, Hirosaki, Aomori 036-8561, Japan.
E-mail: yokoyoko@hirosaki-u.ac.jp
Phone: +81-172-39-3773
FAX: +81-172-39-3773

ORCID ID
Reimi Tada: 0000-0003-4474-1372
Takanori Amano: 0000-0002-0213-4745
Shoma Ishikawa: 0000-0002-6688-0288
Chifuyu Yokoyama: 0000-0002-7476-7496
Saki Nara: 0000-0003-2565-8944
Koshiro Ishida: 0000-0001-6443-4033

Haruki Ochi: 0000-0002-0088-581X
Hajime Ogino: 0000-0003-2707-2330
Nayuta Yakushiji-Kaminatsui: 0000-0001-7324-1161
Yasuhiro Kamei: 0000-0001-6382-1365
Koji Tamura: 0000-0002-1956-2826
Hitoshi Yokoyama: 0000-0003-4821-9506

ABSTRACT

Xenopus young tadpoles regenerate a limb with the anteroposterior (AP) pattern, but metamorphosed froglets regenerate a hypomorphic limb after amputation. The key gene for AP patterning, *shh*, is expressed in a regenerating limb of the tadpole but not in that of the froglet. Genomic DNA in the *shh* limb-specific enhancer, MFCS1 (ZRS), is hypermethylated in froglets but hypomethylated in tadpoles: *shh* expression may be controlled by epigenetic regulation of MFCS1. Is MFCS1 specifically activated for regenerating the AP-patterned limb? We generated transgenic *Xenopus laevis* lines that visualize the MFCS1 enhancer activity with a GFP reporter. The transgenic tadpoles showed GFP expression in *hoxd13*- and *shh*-expressing domains of developing and regenerating limbs, whereas the froglets showed no GFP expression in the regenerating limbs despite having *hoxd13* expression. Genome sequence analysis and co-transfection assays using cultured cells revealed that Hoxd13 can activate *Xenopus* MFCS1. These results suggest that MFCS1 activation correlates with regeneration of AP-patterned limbs and that re-activation of epigenetically inactivated MFCS1 would be crucial to confer the ability to non-regenerative animals for regenerating a properly patterned limb.

INTRODUCTION

Among tetrapods, only urodele amphibians (newts and salamanders) can regenerate an amputated limb completely throughout their life cycles (Han et al., 2005; Joven et al., 2019; Otsuki and Tanaka, 2022; Agata and Inoue, 2012). In the anuran amphibian *Xenopus laevis*, a tadpole can completely regenerate its limbs prior to the onset of metamorphosis, but it loses regenerative capacity gradually as metamorphosis proceeds (Dent, 1962; Muneoka et al., 1986). The froglet, a young post-metamorphosis adult, regenerates only an unbranched cartilaginous spike-like structure after limb amputation (Dent, 1962; reviewed in Suzuki et al., 2006): the spike lacks the pattern formation along the anteroposterior (AP) axis. In the limb formation process, *sonic hedgehog* (*shh*) is expressed in the posterior part of the limb bud and serves as the key gene for the AP axis formation (Riddle et al., 1993; Harfe et al., 2004). *shh* is also expressed in the posterior part of a regenerating limb (blastema) in urodeles (Imokawa and Yoshizato, 1997; Torok et al., 1999). In *Xenopu*s, *shh* is expressed in the posterior part of the limb blastema of a tadpole (Endo et al., 1997) but is not expressed in the blastema of a froglet limb (Endo et al., 2000; Yakushiji et al., 2007). Treatment with a Hedgehog inhibitor results in hypomorphic limb regeneration in both a *Xenopus* tadpole and an axolotl (Roy and Gardiner, 2002; Satoh et al., 2006). These results suggest that *shh* re-expression correlates with the limb regenerative capacity: whether a limb regenerates with the AP pattern or not.

Genetic studies in mice have revealed that a long-range cis-acting enhancer called MFCS1 (mammal-fish-conserved-sequence 1), also called ZRS (ZPA regulating sequence) or Rr29, regulates limb-specific *Shh* expression (Lettice et al., 2003; Sagai et al., 2004). In transgenic (Tg) mouse embryos, MFCS1 with a minimal promoter drives *lacZ* expression in the posterior part of a limb bud (Lettice et al., 2003). Depletion of a large part of this sequence in a mouse results in limb-specific loss of *shh* expression and in loss of the AP polarity of a limb (Sagai et al., 2005). The activity of MFCS1 is positively regulated by Hoxd13 (5' Hoxd) and ETS transcription factors (ETS1 and GABPα), downstream factors of FGF signaling in a mouse limb bud that directly bind to MFCS1 (Capellini et al., 2006; Lettice et al., 2012). In amphibian limbs, the methylation level of genomic DNA in MFCS1 is relatively high in the limbs (both intact and

120 regenerating limbs) of a *Xenopus* froglet, while the methylation level is low to medium
121 in the limbs of a *Xenopus* tadpole, an axolotl and a Japanese newt (Yakushiji et al., 2007).
122 These findings strongly suggest that epigenetic inactivation of MFCS1 leads to the
123 shutdown of *shh* expression that results in hypomorhic limb regeneration without the AP
124 pattern in a froglet. The importance of MFCS1 for limb regeneration is further supported
125 by the results of partial deletion of the MFCS1 sequence by CRISPR/Cas9 in an Iberian
126 ribbed newt: the partial deletion resulted in reduction in *shh* expression and reduction in
127 the number of digits in limb regeneration (Suzuki et al., 2018). However, the spatio-
128 temporal activation pattern of MFCS1 has not been visualized in regenerating limbs of
129 amphibians. Thus, it is still unknown whether MFCS1 is activated in regenerating limbs
130 of amphibians.

131 Here, we succeeded in visualizing and monitoring the spatio-temporal pattern of
132 MFCS1 activation in regenerating limbs as well as in developing limbs by establishing
133 Tg *Xenopus laevis* lines carrying a GFP reporter linked to MFCS1 (MFCS1-GFP).
134 Expression patterns of MFCS1-GFP were overlapped with those of *shh* both in limb
135 development and limb regeneration. MFCS1-GFP expression was specifically localized
136 in the regenerating limb of a young tadpole. The pattern of MFCS1-GFP expression
137 coincided with the expression pattern of *hoxd13* in both developing and regenerating
138 tadpole limbs. Furthermore, genome sequence analysis and luciferase assays *in vitro*
139 suggested a positive regulation of *Xenopus* MFCS1 by Hoxd13. However, despite *hoxd13*
140 expression, MFCS1-GFP expression was not found in the regenerating froglet limb. We
141 revealed that the DNA methylation level of exogenous MFCS1 of the transgene as well
142 as that of endogenous MFCS1 in the limb were higher in the froglet than in the tadpole.
143 Our results suggest that MFCS1 is activated in limb regeneration with the AP pattern but
144 is inactivated in hypomorphic limb regeneration after metamorphosis when MFCS1 has
145 a higher DNA methylation status than that in tadpole stages.
146

147 ## RESULTS AND DISCUSSION

148 **MFCS1-GFP expression localizes in the posterior mesenchyme of a developing limb**
149 **bud**

150 To visualize the MFCS1 activity by the GFP reporter, we generated a transgene construct

151 containing GFP immediately downstream of a *Xenopus shh* promoter sequence
152 (Yakushiji et al., 2007) (Fig. 1A). At the same time, an approximately 3.2-kbp *Xenopus*
153 MFCS1 sequence was cloned and inserted upstream of the *shh* promoter in the transgene
154 construct (Fig. 1A). We generated transgenic *X. laevis* containing this transgene named
155 "*Xla.Tg(Xtr.shh:GFP)*^{Tamura}" (according to the Xenbase nomenclature guideline). For
156 simplicity and for highlighting the involvement of the limb-specific enhancer, MFCS1,
157 we hereafter refer to this Tg as MFCS1-GFP. We observed the GFP pattern in G0 founder
158 animals. Since *shh* is most prominently expressed in the posterior part of a limb bud at
159 stage 51-52 (Endo et al., 1997; Fig. 1B), we firstly focused on limb buds at stage 51-52
160 (Nieuwkoop and Faber, 1994). GFP was found in the posterior part of the limb bud in at
161 least eleven independent G0 individuals and the fluorescence gradually diminished after
162 stage 52. Thus, we considered that the pattern of MFCS1-GFP expression reflects the
163 activity of the MFCS1 enhancer. We established two independent lines by mating selected
164 GFP-expressing founder animals with wild-type frogs (Table S1). About 50% of the N1
165 individuals of line 2 as well as the N1 and N2 individuals of line 1 were GFP-positive in
166 limb buds, presumably being inherited in a Mendelian manner. Consistent with G0
167 animals, limb buds of both line 1 and line 2 at stage 51-52 showed GFP expression in the
168 posterior part (Fig. 1C, C' and Fig. S1A, A'). In the following experiments, we used GFP-
169 positive individuals of line 1 (N1 or N2) and line 2 (N1).

170 Confocal imaging revealed that GFP was localized specifically in the posterior
171 mesenchyme of the limb bud at stage 51-52 (Fig. 1D, E and Fig. S1B, C). In limb
172 development, GFP was firstly observed at stage 50 around the apical tip of a limb bud
173 (Fig. 1F, F' and Fig. S1D, D'). This observation is consistent with the initial weak *shh*
174 expression detected at stage 50 by whole mount *in situ* hybridization (Endo et al., 1997).
175 GFP expression became strongest at stages 51 and 52 and the fluorescence was more
176 posteriorly polarized by stage 52 (Fig. 1G, G', H, H' and Fig. S1E, E', F, F'). At stage 53,
177 GFP was found in the distal-posterior part of the limb bud (Fig. 1I, I' and Fig. S1G, G')
178 and the fluorescence was weaker than that at stage 52. Finally GFP expression was almost
179 undetectable at stage 54 (Fig. 1J, J' and Fig. S1H, H'). These observations were, in
180 principle, consistent with the spatio-temporal *shh* expression patterns (Endo et al., 1997),
181 while the domain of GFP expression appeared to be broader than that of *shh* expression.
182 We concluded that the MFCS1-GFP expression pattern in the Tg lines mostly visualizes

183 the activity of the endogenous MFCS1 enhancer in a developing limb bud.
184
185 **MFCS1-GFP expression predicts the AP duplication of a limb bud**
186 To further examine whether MFCS1-GFP expression correlates with limb morphogenesis
187 along the AP axis, we conducted a 180° rotation experiment on limb buds of Tg (line 1)
188 tadpoles (Fig. 2A). Cameron and Fallon (1977) found limb duplication along the AP axis
189 after rotation of the distal limb bud tips 180° on the proximo-distal axis at stage 51-53 in
190 *X. laevis*. Endo et al. (1997) repeated this experiment at stage 53 and found that ectopic
191 *shh* expression was induced in the posterior region of the graft and stump. To test the
192 correlation between MFCS1 enhancer activity and limb duplication along the AP axis,
193 we repeated this experiment and examined the GFP expression pattern (Fig. 2). Consistent
194 with the preceding results in control limb buds, in which the amputated distal tip of each
195 limb bud was returned to the stump in the original orientation, showing only faint ectopic
196 *shh* expression (Endo et al., 1997), the majority of the control limb buds (ten of 12
197 samples) without rotation did not show GFP expression and did not result in limb
198 duplication (Fig. 2B, C). In contrast, the majority of 180° rotated limb buds (eight of 11
199 samples) showed ectopic induction of GFP expression in the posterior part of the distal
200 limb bud tip (graft) and finally formed duplicated limbs along the AP axis (the number
201 of digits in a limb being more than 5) (Fig. 2D-G). These results (summarized in Table
202 S2) suggest that ectopic induction of MFCS1 activity is closely related to ectopic *shh*
203 expression and subsequent limb duplication along the AP axis, further suggesting that
204 MFCS1-GFP expression faithfully reflects the endogenous *shh* enhancer activity in a
205 limb.
206
207 **MFCS1 is activated in a blastema that regenerates a limb with the AP pattern.**
208 To examine whether MFCS1 is activated in limb regeneration with the AP pattern, we
209 amputated a stage 54 limb bud at the level of the presumptive ankle: this amputation
210 results in almost complete limb regeneration along the AP axis (Muneoka et al., 1986).
211 By this stage, *shh* expression and MFCS1-GFP expression in an intact limb bud have
212 become almost undetectable by *in situ* hybridization and observation under a fluorescence
213 stereomicroscope, respectively (Fig. 1 and Fig. S1) (Endo et al., 1997). At 4 days post
214 amputation (dpa), GFP was observed broadly in the regenerating blastema (Fig. 3R and

215 Fig. S2B-B''), indicating that MFCS1 is re-activated in the blastema that regenerates a
216 well-patterned limb.
217 MFCS1-GFP expression was distributed throughout the blastema and did not
218 appear to be localized posteriorly. It became stronger at 6 dpa (Fig. S2C-C'') and the
219 expression gradually diminished after the blastema showed a pallet shape and became
220 undetectable at 10 dpa (Fig. 3S, T and Fig. S2). *shh* expression was detected in the
221 posterior part of a blastema at 4 dpa by *in situ* hybridization (Fig. 3E). Based on these
222 results, we judged that MFCS1-GFP expression is distributed broadly in regenerating
223 blastemas and that the temporal expression pattern of MFCS1-GFP coincidences with
224 that of *shh* expression, while the spatial MFCS1-GFP expression pattern is wider than the
225 *shh*-expressing domain. MFCS1-GFP signal in the regenerating blastema of a young
226 tadpole suggests that MFCS1 is re-activated in a regenerating limb with the AP pattern
227 formation when *shh* is expressed: *shh* expression in the regenerating limb as well as in
228 the developing limb seems to be regulated by the common enhancer, MFCS1.
229
230 **MFCS1-GFP expression pattern correlates with the pattern of *hoxd13* expression in**
231 **a tadpole**
232 Hoxd13 and FGF downstream factors, ETS transcription factors, positively regulate the
233 MFCS1 enhancer in mice (Capellini et al., 2006; Lettice et al., 2012). We examined *dusp6*
234 (*mkp3*) expression and *hoxd13* expression as indicators of positive upstream regulators
235 of MFCS1. *dusp6* expression is induced by FGF signaling (Eblaghie et al., 2003;
236 Kawakami et al., 2003) and it seems to reflect the activity of downstream factors of FGF
237 signaling, especially ETS transcription factors (Ekerot et al., 2008). We chose a stage 51
238 limb bud and a 4 dpa blastema of a tadpole in which the limb bud was amputated at the
239 presumptive ankle level at stage 54 as representatives of developing and regenerating
240 limbs, respectively: both initiate prominent *shh* expression in the posterior side (Fig. 3E,
241 I). In a developing limb bud, *dusp6* is expressed broadly in a limb bud and strong
242 expression is seen especially in the apical mesenchyme (Fig. 3K). *hoxd13* is expressed in
243 the posterior mesenchyme of a limb bud (Fig. 3L) and its expression domain is wider than
244 the *shh*-expressing domain (Fig. 3I). The posterior mesenchymal region of a limb bud is
245 positive for both *dusp6* and *hoxd13* and the double positive region seems to coincide with
246 the fluorescence of MFCS1-GFP (Fig. 1C', D, G') and *gfp* transcript (Fig. 3J) patterns.

247 The *gfp* transcript was not detected in line 2 limb bud samples (n=0/6) but was detected
248 in line 1 limb bud samples (n=10/10) by *in situ* hybridization, suggesting that line 1 has
249 stronger transgene expression than that of line 2. The coincidence between upstream
250 regulators and MFCS1-GFP expression seems to be clearer in a regenerating limb: *dusp6*
251 (Fig. 3G) and *hoxd13* (Fig. 3H) were strongly expressed in whole region of a blastema.
252 MFCS1-GFP expression (Fig. 3R) and *gfp* transcript expression (Fig. 3F) are robustly
253 distributed in the entire blastema, while *shh* expression is restricted to the posterior edge
254 of the blastema (Fig. 3E). Therefore, the MFCS1-GFP expression domain is larger than
255 the *shh* expression domain, especially in a regenerating limb. Transcriptional repression
256 by a silencer or defined regulation of chromatin conformational change resulting in the
257 proximity of MFCS1 and the *shh* promoter (Amano et al., 2009) may further restrict
258 endogenous *shh* expression to the posterior edge of the blastema. Even though *shh*
259 expression is spatially narrower than the GFP expression pattern, the expression pattern
260 of MFCS1-GFP covers the *shh*-expressing domain and coincides with the expression
261 domains of upstream regulators represented by *hoxd13* and *dusp6*.
262

263 **MFCS1 is inactive in a limb blastema of a metamorphosed froglet despite *hoxd13***
264 **expression**

265 In contrast to a young tadpole, a limb of a metamorphosed froglet does not express *shh*
266 after amputation, and amputation results in regeneration of a cartilaginous spike, while
267 an amputated limb of a froglet forms a regeneration blastema (Endo et al., 2000; Suzuki
268 et al., 2006; Yakushiji et al., 2007). Hypermethylated status of genomic DNA at the
269 MFCS1 enhancer strongly suggested that this enhancer is inactivated in a froglet limb:
270 the enhancer inactivation implies transcriptional inactivation of *shh* in the limb (Yakushiji
271 et al., 2007). To examine whether inactivation of the enhancer occurs after
272 metamorphosis, we examined MFCS1-GFP expression in limb regeneration of a froglet.
273 From the early stage (early bud) blastema to the late stage rod-shaped blastema, no
274 specific GFP was observed in the blastema, while non-specific fluorescence was
275 sometimes observed in both MFCS1-GFP Tg froglets and wild-type ones (controls) (Fig.
276 3M-P and Fig. S3). Therefore, we conclude that MFCS1 is inactivated completely or is
277 much more inactive in the blastema of a froglet limb than in that of a young tadpole.
278 We then examined expression of upstream regulators of MFCS1. By 10 dpa, an

279 amputated limb of a froglet forms a cone-shaped blastema and the blastema already starts
280 expressing *fgf-8*, *fgf-10*, *msx1*, and *hand2,* genes that are involved in maintenance/
281 induction of *shh* expression in a limb bud (Suzuki et al., 2005; Yakushiji et al., 2007). In
282 addition, Yakushiji et al. (2007) reported hypermethylation status of genomic DNA in a
283 limb blastema at 10 dpa in a froglet. Therefore, we chose blastema at 10 dpa and examined
284 gene expression at that time point. Similar to the results of a study by Satoh et al. (2006)
285 for the blastema at a later time point (14 dpa), *hoxd13* was broadly expressed in the
286 blastema at 10 dpa (Fig. 3D). *dusp6* was also expressed in the blastema (Fig. 3C), while
287 no *shh* (and *gfp*) expression was detected in the blastema as Yakushiji et al. (2007)
288 reported previously (Fig. 3A, B). The expression of *hoxd13* and *dusp6* in a froglet
289 blastema suggests that upstream regulators of MFCS1 (5' Hoxd and ETS transcription
290 factors) as well as *hand2* (Yakushiji et al., 2007) are not absent in the froglet blastema.
291 Thus, MFCS1 in a froglet limb appears to be unable to respond to positive regulators
292 represented by Hoxd13.
293
294 **Higher DNA methylation level of MFCS1 may inactivate the enhancer's**
295 **responsiveness to Hoxd13 in a froglet limb**
296 To confirm the potential responsiveness of MFCS1 to the upstream regulators, we
297 conducted luciferase assays *in vitro* using MFCS1 with the *shh* promoter. The *luc2*
298 reporter under control of the MFCS1 enhancer with either *shh* or a minimum promoter
299 (Fig. 4A, upper diagram) was prepared. A local alignment of the highly conserved
300 sequences from different species revealed that there are multiple putative Hox-binding
301 motifs in the conserved sequences (Fig. 4A, see also Fig. S4). The full lengths of *Hoxd13*,
302 *Fgf2*, *Fgf4*, and *Fgf8* were flanked with the CMV promoter as gene expression constructs.
303 MFCS1-*shh* promoter-*luc2* or MFCS1-minP-*luc2* reporter constructs were co-transfected
304 with various combinations of the gene expression constructs into NIH3T3 cells. The
305 reporter activities of cells transfected with MFCS1-shh promoter-*luc2* were significantly
306 increased when co-transfecting with *Fgf2* (1.4-fold vs. mock), *Fgf4* (1.5-fold vs. mock),
307 *Fgf8* (1.3-fold vs. mock), or *Hoxd13* (2.3-fold vs. mock) (Fig. 4B). The combination of
308 *Fgf4* and *Hoxd13* additively affected MFCS1-driven gene activation (1.1-fold vs. *Hoxd13*
309 alone). Meanwhile, transfection of the MFCS1-*luc2* construct containing minP had did
310 not result in significant activation of the luciferase reporter even in the presence of any

311 expression constructs. When the MFCS1-*luc2* was artificially methylated by CpG
312 methyltransferase (M.SssI) in advance, the responsiveness of the reporter to Hoxd13 was
313 strongly suppressed by ~260 fold (Fig. S5). Taken together with the highly methylated
314 status of MFCS1 in a *Xenopus* froglet limb (Yakushiji et al., 2007), this result raises the
315 possibility that DNA methylation of MFCS1 inactivates its responsiveness to Hoxd13.
316 Genomic DNA methylation leads to chromatin condensation, inhibits access of
317 transcription factors to the enhancer sequence and finally results in transcriptional
318 repression (Bird and Wolffe, 1999). To further examine whether a high methylation level
319 of MFCS1 exerts a suppressive effect on gene expression, we investigated the
320 methylation status of MFCS1 as the transgene in MFCS1-GFP Tg tadpoles and froglets.
321 Within an MFCS1 highly conserved sequence in amphibians, there are nine CpG sites
322 both in *X. tropicalis* and *X. laevis* (Fig. S6). Firstly, we examined DNA methylation status
323 of MFCS1 in wild-type tadpoles and froglets by bisulfite sequencing as reported by
324 Yakushiji et al. (2007) and obtained consistent results: While limb buds of young tadpoles
325 have a lower methylation level (26.3%), froglet limbs have a higher methylation level
326 (87.2%) as shown in Fig. 4C. We then examined the methylation level of the MFCS1
327 sequence as the transgene in MFCS1-GFP Tg (line 1). Again, froglet limbs have a higher
328 methylation level (17.2%) than that in limb buds of young tadpoles (2.6%) (Fig. 4C).
329 After limb amputation in a froglet and after completion of spike regeneration, a higher
330 methylation level than that in tadpoles was still found in the Tg regenerates (line 1,
331 14.4%) (Fig. S7). The nine CpG sites in MFCS1 (highly conserved sequence in
332 amphibians) as the transgene were susceptible to methylation to some extent also in line
333 2 (Fig. S7). Although the basal methylation level differs between endogenous MFCS1
334 and transgene MFCS1, the increase in the methylation level of the transgene MFCS1 after
335 metamorphosis also correlated with the ontogenetic inactivation of gene expression under
336 control of the enhancer.
337
338 **Conclusions**
339 In this study, we visualized MFCS1 activity in limb regeneration of an amphibian.
340 MFCS1-GFP Tg *Xenopus* revealed that MFCS1 enhancer is re-activated specifically in
341 the regenerating blastema for a patterned limb in a young tadpole but not in the blastema
342 for a hypomorphic limb in a froglet. MFCS1 seems to be activated by Hoxd13 in a tadpole

343 but seems to be unable to respond to Hoxd13 in a froglet. An ontogenetic increase in the
344 MFCS1 methylation level may block the function of Hoxd13 (and other positive
345 regulators) as a transcriptional activator(s) to the enhancer so that transcription of a gene
346 under control of the enhancer is inactivated (Fig. 4D). For improvement of regenerative
347 capacity in a froglet limb by re-activation of *shh* expression, removal of epigenetic
348 silencing of MFCS1 would be important. The combinational application of an inhibitor
349 of DNA methyltransferase and a histone deacetylase inhibitor stimulated *shh* expression
350 in cultured blastema cells of a froglet limb in a previous *in vitro* study (Yakushiji et al.,
351 2009), suggesting that application of such reagents affecting epigenetic modification
352 could be hopeful if the treatment condition is optimized *in vivo*. As an alternative
353 approach, CRISPR-based epigenome editing that removes DNA methylation (e.g., Nuñez
354 et al., 2021) may be effective. In these approaches, the MFCS1-GFP Tg line would be
355 useful for evaluating the effectiveness. The enhancer activation is easily detected by GFP
356 and it would thus be possible to screen chemicals that remove epigenetic silencing of the
357 enhancer in a large scale. If regeneration of a well-patterned limb is induced in a froglet
358 by re-activation of MFCS1, it would be a precious model case for recovery of organ-level
359 regeneration in non-regenerative higher vertebrates by manipulating epigenetics.
360

361 # MATERIALS AND METHODS

362 **Transgene construction and *in situ* hybridization**

363 A 3,164-bp MFCS1 enhancer sequence was amplified from *Xenopus tropicalis* genomic
364 DNA prepared from a Nigerian line with primers (XtMFCS1-Fw and Xt-MFCS1-Rv;
365 Table S3). The PCR product was cloned into the pCRII-TOPO vector (Invitrogen) and
366 sequenced. The *Xenopus laevis shh* promoter (Yakushiji et al., 2007) was cloned into a
367 reporter construct that contains an EGFP expression cassette. Then the MFCS1-*shh*
368 promoter-*egfp* was generated by inserting the 3,164-bp MFCS1 enhancer sequence
369 upstream of the *shh* promoter (Fig. 1A). For synthesis of probes for *in situ* hybridization,
370 a *hoxd13* cDNA clone, BC080434, inserted in pCMV-SPORT6 was obtained from
371 Dharmacon. The *hoxd13*/ pCMV-SPORT6 plasmid was linearized with SalI and
372 transcribed with T7 RNA polymerase. DIG-labeled RNA probes of *hoxd13*, *shh* (Endo et
373 al., 1997), *gfp* (Hayashi et al., 2015) and *dusp6* (Gomez et al., 2005) were prepared

374 according to the protocol of the manufacturer (Roche). To prepare serial cryosections, the
375 specimens were fixed in MEMFA (0.1 M MOPS at pH 7.4, 2 mM EGTA, 1 mM $MgSO_4$,
376 3.7% formaldehyde) overnight at room temperature, embedded in OCT compound
377 (Sakura), and serially sectioned at 8-10 µm by a cryostat. *In situ* hybridization on frozen
378 sections was performed according to Yoshida et al. (1996) with slight modifications.
379 Sections were observed under an upright microscope (Olympus BX53) with an objective
380 lens (Olympus UPlan PLN 10X) and were photographed by a digital camera (Leica
381 DFC7000T).
382
383 **Animal husbandry and transgenesis in *Xenopus laevis***
384 Wild-type *Xenopus laevis* adult frogs were purchased from domestic animal venders,
385 Watanabe Zoushoku (http://www5d.biglobe.ne.jp/~zoushoku/top.htm) and Hamamatsu
386 Seibutsu Kyozai (http://www.h-seibutsu.co.jp/index.html). Founder (G0) MFCS1-GFP
387 Tg *Xenopus laevis* embryos were generated by a REMI technique (Kroll and Amaya,
388 1996) using oocyte extract instead of egg extract (Hirsch et al., 2002; reviewed in Ogino
389 and Ochi, 2009). MFCS1-GFP N1 Tg *Xenopus laevis* lines were obtained by crossing
390 sexually mature MFCS1-GFP G0 frogs with wild-type frogs. Tadpoles and froglets were
391 reared at 22–23°C in dechlorinated tap water. The rearing containers were cleaned daily,
392 and the tadpoles were fed powdered barley grass (Odani Kokufun, Japan or Yamamoto
393 Kanpoh, Japan). At stage 58 (Nieuwkoop and Faber, 1994), the feeding was ceased until
394 metamorphosis was completed. After metamorphosis, the froglets were fed dried tubifex
395 every other day. All surgery was performed under ethyl-3-aminobenzoate anesthesia, and
396 all efforts were made to minimize suffering. When tadpoles and froglets needed to be
397 euthanized, they were immersed in 0.05% ethyl-3-aminobenzoate (Tokyo Chemical
398 Industry, 886-86-2). When adult male frogs were sacrificed to excise their testes for
399 transgenesis, 2% ethyl-3-aminobenzoate dissolved in pure water was injected into the
400 intracardiac cavity (400 µg of ethyl-3-aminobenzoate/1 g of animal). After the male frog
401 was confirmed to be completely unconscious, its testes were excised with a blade, and
402 then the unconscious frog was put in a freezer for euthanization. All animal care and
403 experimentation procedures were conducted in accordance with the animal care and use
404 committee guidelines of Tohoku University (2015LsA-023) and Hirosaki University
405 (A15003, A15003-1).

406

407 **Observation of developing and regenerating limbs, limb amputation and 180°**
408 **rotation of a limb bud**

409 For observation of limb development and limb regeneration in tadpoles, we used hindlimb
410 buds since it is much easier to observe and to operate on hindlimb buds than forelimb
411 buds due to their size and accessibility. To observe the regenerating limb bud (blastema)
412 of a tadpole, tadpoles at stage 54 were anesthetized with 0.025% ethyl-3-aminobenzoate
413 and hindlimb buds were amputated using ophthalmologic scissors at the presumptive
414 ankle level (according to the outside view and a fate map by Tschumi, 1957). For
415 preparation of a 180° rotated limb bud, Nile Blue A particles were embedded into the
416 anterior side of the distal tip of a stage 53 hindlimb bud with a tungsten needle as the
417 reference point indicating the original AP axis of the graft according to Cameron and
418 Fallon (1977). Subsequently, the limb bud was amputated at the presumptive ankle level
419 (Tschumi, 1957) and then the distal limb bud tip was rotated 180° (not rotated for control
420 limbs) on the proximo-distal axis, returned to the stump, and fixed with tungsten pins
421 according to Cameron and Fallon (1977) and Endo et al. (1997). After metamorphosis,
422 the resulting limbs were fixed in 10% formalin in Holtfreter's solution and stained with
423 0.1% Alcian blue as previously reported (Yokoyama et al., 1998). Then digit identity was
424 determined by the number of phalanges in association with the presence/absence of a
425 claw (Cameron and Fallon, 1977). To observe the blastema of a froglet, froglets were
426 anesthetized with 0.05% ethyl-3-aminobenzoate and then forelimbs were amputated
427 through the distal zeugopodium with ophthalmologic scissors and the amputation surface
428 was trimmed to be flat. For observation of limb regeneration in froglets, we used
429 forelimbs since hindlimb amputation often results in drowning of the froglets.

430

431 **Imaging of whole-mount limb samples**

432 Tadpoles and froglets anesthetized with 0.025% or 0.05% ethyl-3-aminobenzoate were
433 observed under a fluorescence stereomicroscope (Nikon SMZ18) with a 0.5x objective
434 lens using a GFP longpass filter (if in a fluorescent view) and photographed by a digital
435 camera (Olympus DP74 or DP73). For confocal microscopy (Fig. 1D, E and Fig. S1B,
436 C), anesthetized tadpoles were each placed on a 35-mm glass-bottom dish (Iwaki, Japan)
437 so that the dorsal surface of the hindlimb bud was tightly attached to the glass-bottom.

The prepared samples were observed under an FV3000 confocal laser scanning microscope (Olympus) equipped with an Olympus UPlanSApo 20× dry objective lens. Fluorescence between 500 nm and 600 nm was detected by a GaAsP photo multiplier tube.

Genome sequence analysis

The 449-b genomic sequences corresponding to a conserved core region of human MFCS1 (hg38, chr7: 156,791,242－156,791,690) and its orthologous sequences in the mouse (mm39, chr5: 29,520,033–29,520,474), chicken (galGal6, chr2: 8,553,351–8,553,801), *X. tropicalis* (xenTro10, chr6: 17,346,249–17,346,700) and *X. laevis* (J-strain 10.1, Chr6L: 15,900,483–15,900,931) were downloaded from the UCSC Genome Browser and Xenbase (Karolchik et al., 2003; Fortriede et al., 2020). These sequences were aligned using MUSCLE (Edgar, 2004). Searches for potential transcription factor-binding sites were performed with transcription factor-binding motifs collected from the TRANSFAC and JASPAR databases (Wingender, 2008; Castro-Mondragon et al., 2022). The *X. tropicalis* MFCS1 element used for our functional analyses contains a 12-thymidine repeat in place of the 14-thymidine repeat underlined in the alignment (Fig. 4A, underlined). This difference may be because of a polymorphism between the strain used for our study and that used for the genome sequencing project (Igawa et al., 2015).

Reporter construction, cell culture and luciferase assay

The highly conserved 998-bp core sequence of *Xenopus tropicalis* MFCS1 was amplified by PCR with specific primers (Table S3) and inserted into the Acc65I and XhoI sites of the pGL4.23 vector (Promega, E8411). Then the minimal promoter of the pGL4.23 vector was replaced with a 486-bp sequence of *Xenopus laevis shh* promoter (Fig. 4A). It should be noted that the 14-thymidine repeat in *X. tropicalis* MFCS1 sequence from the UCSC Genome Browser (Fig. 4A, underlined) was shortened to a 12-thymidine repeat in the transgene construct (Fig. S6) and the reporter construct for the luc assay. pGL4.74 containing the *Renilla* luciferase gene was used for normalization of reporter expression (Promega, E6921). Coding sequences of mouse *Hoxd13*, *Fgf2*, *Fgf4* and *Fgf8* were cloned into the pcDNA3.1 vector (ThermoFisher, V79020). NIH3T3 cell line (RCB2767) was

469 obtained from the RIKEN BioResource Research Center. NIH3T3 cells were maintained
470 in Dulbecco's modified Eagle's medium (ThermoFisher, 11960-044) containing 10%
471 fetal bovine serum, 1x GlutaMax and 100 μg/ml penicillin–streptomycin. Cells at 70–
472 90% confluency were transfected with equal amounts of luciferase reporter and gene
473 expression plasmids using Lipofectamine 3000 (ThermoFisher). Luciferase activity in the
474 cell lysates was measured using a Dual-Luciferase Reporter Assay System (Promega)
475 according to the manufacturer's protocol. For statistical analysis, Student's *t*-tests (two-
476 tailed) were applied when equal variance tests were passed.
477
478 **Bisulfite genomic sequencing**
479 Presumptive autopods of hindlimb buds (Tschumi, 1957) from thirty-five wild-type and
480 sixteen MFCS1-GFP Tg (line 1) tadpoles at stage 54 were collected. Forelimb autopods
481 from five wild-type and six MFCS1-GFP Tg (line 1) froglets were collected. Spike
482 regenerates from two MFCS1-GFP Tg (line 1) and two same Tg (line 2) frogs were
483 collected. Then genomic DNA was extracted from these tissue samples. The genomic
484 DNA was treated with sodium bisulfite using an EZ DNA Methylation-Gold Kit
485 following the protocol of the manufacturer (Zymo Research). DNA was amplified by 30
486 cycles of a three-step PCR (98°C for 10 sec, 60°C for 30 sec and 68°C for 30 sec) with
487 MFCS1_BS_Fw and MFCS1_BS_Rv primers (Table S3) using KOD -Multi & Epi-
488 (Toyobo). Each product was cloned into the pANT vector (Nippon Gene) or pGEM-T
489 easy (Promega) and sequenced with M13F-pUC or M13R-pUC primers (Table S3).
490

491 ## ACKNOWLEDGMENTS

492 We thank Yoshiko Yoshizawa and Natsume Sagawa for excellent animal care. We thank
493 Drs. Makoto Asashima, Shuji Takahashi and Yoshio Yaoita for providing the Nigerian
494 line of *X. tropicalis*. We thank Dr. Ikuo Uchiyama for support in gene expression analysis.
495 This work was partially supported by the NIBB Collaborative Research Program to HY
496 (19-451, 20-436, 21-307, 21-401). This work was supported by the National Bio-
497 Resource Project (NBRP) of the MEXT, Japan. We acknowledge Shared Facility Center
498 for Science and Technology, Hirosaki University (SFCST) for confocal microscope
499 observation by FV3000 (Olympus). We thank Dr. Chisato Ushida, Dr. Michiko Sasabe,

Shunsuke Hosoi, Misako Saida and Hibiki Yokoyama for their help in using confocal microscopy. We thank Dr. Daisuke Kurita for help in TA cloning. We thank Drs. Gembu Abe and Kazuya Kobayashi for their help in preparation of tungsten needles. We thank Dr. Jose F. de Celis for providing *Xenopus laevis dusp6* cDNA.

Competing interests

The authors declare no competing or financial interests.

Author contributions

Conceptualization: K.T., H.Y.; Methodology: T.A., N.Y.-K., J.S., Y.K., H.Y.; Validation: T.A., N.Y.-K., H.Y.; Formal analysis: T.A., H.Ogino, H.Y.; Investigation: R.T., T.H., T.A., S.I., C.Y., S.N., K.I., A.K., H.Ochi, H.Ogino, N.Y.-K., Y.K., H.Y.; Resource: T.A., A.K., H.Ochi, H.Ogino, N.Y.-K., Y.K., K.T., H.Y.; Writing – original draft preparation: T.A., H.Ogino, J.S., Y.K., H.Y.; Writing – review and editing: A.K., H.Ochi, H.Ogino, N.Y.-K., K.T., H.Y.; Visualization: R.T., T.H., T.A., S.I., H.Ogino, N.Y.-K., H.Y.; Supervision: K.T., H.Y.; Project administration: H.Ogino, K.T., H.Y.; Funding acquisition: K.T., H.Y.

Funding

H.Y is funded by MEXT and JSPS KAKENHI (grant number 22124005). H.Y. is funded by JSPS KAKENHI (grant number 16H04790, 21K06195). H.Y. is funded by Grant for Basic Science Research Projects from The Sumitomo Foundation. H.Y is funded by Hirosaki University Institutional Research Grant for Young investigators.

REFERENCES

Agata, K. and Inoue, T. (2012). Survey of the differences between regenerative and non-regenerative animals. *Dev Growth Differ* **54**, 143-152.

Amano, T., Sagai, T., Tanabe, H., Mizushina, Y., Nakazawa, H. and Shiroishi, T. (2009). Chromosomal dynamics at the Shh locus: limb bud-specific differential regulation of competence and active transcription. *Dev Cell* **16**, 47-57.

Bird, A. P. and Wolffe, A. P. (1999). Methylation-induced repression--belts, braces, and chromatin. *Cell* **99**, 451-454.

Cameron, J. A. and Fallon, J. F. (1977). Evidence for polarizing zone in the limb buds of Xenopus laevis. *Dev Biol* **55**, 320-330.

Capellini, T. D., Di Giacomo, G., Salsi, V., Brendolan, A., Ferretti, E., Srivastava, D., Zappavigna, V. and Selleri, L. (2006). Pbx1/Pbx2 requirement for distal

535 limb patterning is mediated by the hierarchical control of Hox gene spatial
536 distribution and Shh expression. *Development* **133**, 2263-2273.
537 **Castro-Mondragon, J. A., Riudavets-Puig, R., Rauluseviciute, I., Lemma, R. B.,**
538 **Turchi, L., Blanc-Mathieu, R., Lucas, J., Boddie, P., Khan, A., Manosalva**
539 **Pérez, N., et al.** (2022). JASPAR 2022: the 9th release of the open-access
540 database of transcription factor binding profiles. *Nucleic Acids Res* **50**, D165-
541 D173.
542 **Dent, J. N.** (1962). Limb regeneration in larvae and metamorphosing individuals of the
543 South African clawed toad. *J Morphol* **110**, 61-77.
544 **Eblaghie, M. C., Lunn, J. S., Dickinson, R. J., Münsterberg, A. E., Sanz-Ezquerro,**
545 **J. J., Farrell, E. R., Mathers, J., Keyse, S. M., Storey, K. and Tickle, C.**
546 (2003). Negative feedback regulation of FGF signaling levels by Pyst1/MKP3 in
547 chick embryos. *Curr Biol* **13**, 1009-1018.
548 **Edgar, R. C.** (2004). MUSCLE: multiple sequence alignment with high accuracy and
549 high throughput. *Nucleic Acids Res* **32**, 1792-1797.
550 **Ekerot, M., Stavridis, M. P., Delavaine, L., Mitchell, M. P., Staples, C., Owens, D.**
551 **M., Keenan, I. D., Dickinson, R. J., Storey, K. G. and Keyse, S. M.** (2008).
552 Negative-feedback regulation of FGF signalling by DUSP6/MKP-3 is driven by
553 ERK1/2 and mediated by Ets factor binding to a conserved site within the
554 DUSP6/MKP-3 gene promoter. *Biochem J* **412**, 287-298.
555 **Endo, T., Tamura, K. and Ide, H.** (2000). Analysis of gene expressions during
556 Xenopus forelimb regeneration. *Dev Biol* **220**, 296-306.
557 **Endo, T., Yokoyama, H., Tamura, K. and Ide, H.** (1997). Shh expression in
558 developing and regenerating limb buds of Xenopus laevis. *Dev Dyn* **209**, 227-
559 232.
560 **Fortriede, J. D., Pells, T. J., Chu, S., Chaturvedi, P., Wang, D., Fisher, M. E.,**
561 **James-Zorn, C., Wang, Y., Nenni, M. J., Burns, K. A., et al.** (2020).
562 Xenbase: deep integration of GEO & SRA RNA-seq and ChIP-seq data in a
563 model organism database. *Nucleic Acids Res* **48**, D776-D782.
564 **Gómez, A. R., López-Varea, A., Molnar, C., de la Calle-Mustienes, E., Ruiz-**
565 **Gómez, M., Gómez-Skarmeta, J. L. and de Celis, J. F.** (2005). Conserved
566 cross-interactions in Drosophila and Xenopus between Ras/MAPK signaling and
567 the dual-specificity phosphatase MKP3. *Dev Dyn* **232**, 695-708.
568 **Han, M., Yang, X., Taylor, G., Burdsal, C. A., Anderson, R. A. and Muneoka, K.**
569 (2005). Limb regeneration in higher vertebrates: developing a roadmap. *Anat*
570 *Rec B New Anat* **287**, 14-24.
571 **Harfe, B. D., Scherz, P. J., Nissim, S., Tian, H., McMahon, A. P. and Tabin, C. J.**
572 (2004). Evidence for an expansion-based temporal Shh gradient in specifying
573 vertebrate digit identities. *Cell* **118**, 517-528.
574 **Hayashi, S., Kawaguchi, A., Uchiyama, I., Kawasumi-Kita, A., Kobayashi, T.,**
575 **Nishide, H., Tsutsumi, R., Tsuru, K., Inoue, T., Ogino, H., et al.** (2015).
576 Epigenetic modification maintains intrinsic limb-cell identity in Xenopus limb
577 bud regeneration. *Dev Biol* **406**, 271-282.
578 **Hirsch, N., Zimmerman, L. B., Gray, J., Chae, J., Curran, K. L., Fisher, M.,**
579 **Ogino, H. and Grainger, R. M.** (2002). Xenopus tropicalis transgenic lines and
580 their use in the study of embryonic induction. *Dev Dyn* **225**, 522-535.
581 **Igawa, T., Watanabe, A., Suzuki, A., Kashiwagi, A., Kashiwagi, K., Noble, A.,**

Guille, M., Simpson, D. E., Horb, M. E., Fujii, T., et al. (2015). Inbreeding Ratio and Genetic Relationships among Strains of the Western Clawed Frog, Xenopus tropicalis. *PLoS One* **10**, e0133963.

Imokawa, Y. and Yoshizato, K. (1997). Expression of Sonic hedgehog gene in regenerating newt limb blastemas recapitulates that in developing limb buds. *Proc Natl Acad Sci U S A* **94**, 9159-9164.

Joven, A., Elewa, A. and Simon, A. (2019). Model systems for regeneration: salamanders. *Development* **146**.

Karolchik, D., Baertsch, R., Diekhans, M., Furey, T. S., Hinrichs, A., Lu, Y. T., Roskin, K. M., Schwartz, M., Sugnet, C. W., Thomas, D. J., et al. (2003). The UCSC Genome Browser Database. *Nucleic Acids Res* **31**, 51-54.

Kawakami, Y., Rodríguez-León, J., Koth, C. M., Büscher, D., Itoh, T., Raya, A., Ng, J. K., Esteban, C. R., Takahashi, S., Henrique, D., et al. (2003). MKP3 mediates the cellular response to FGF8 signalling in the vertebrate limb. *Nat Cell Biol* **5**, 513-519.

Kroll, K. L. and Amaya, E. (1996). Transgenic Xenopus embryos from sperm nuclear transplantations reveal FGF signaling requirements during gastrulation. *Development* **122**, 3173-3183.

Lettice, L. A., Heaney, S. J., Purdie, L. A., Li, L., de Beer, P., Oostra, B. A., Goode, D., Elgar, G., Hill, R. E. and de Graaff, E. (2003). A long-range Shh enhancer regulates expression in the developing limb and fin and is associated with preaxial polydactyly. *Hum Mol Genet* **12**, 1725-1735.

Lettice, L. A., Williamson, I., Wiltshire, J. H., Peluso, S., Devenney, P. S., Hill, A. E., Essafi, A., Hagman, J., Mort, R., Grimes, G., et al. (2012). Opposing functions of the ETS factor family define Shh spatial expression in limb buds and underlie polydactyly. *Dev Cell* **22**, 459-467.

Muneoka, K., Holler-Dinsmore, G. and Bryant, S. V. (1986). Intrinsic control of regenerative loss in Xenopus laevis limbs. *J Exp Zool* **240**, 47-54.

Nieuwkoop, P. D. and Faber, J. (1994). *Normal Table of Xenopus laevis (Daudin).* New York: Garland Publishing.

Nuñez, J. K., Chen, J., Pommier, G. C., Cogan, J. Z., Replogle, J. M., Adriaens, C., Ramadoss, G. N., Shi, Q., Hung, K. L., Samelson, A. J., et al. (2021). Genome-wide programmable transcriptional memory by CRISPR-based epigenome editing. *Cell* **184**, 2503-2519.e17.

Ogino, H. and Ochi, H. (2009). Resources and transgenesis techniques for functional genomics in Xenopus. *Dev Growth Differ* **51**, 387-401.

Otsuki, L. and Tanaka, E. M. (2022). Positional Memory in Vertebrate Regeneration: A Century's Insights from the Salamander Limb. *Cold Spring Harb Perspect Biol* **14**.

Riddle, R. D., Johnson, R. L., Laufer, E. and Tabin, C. (1993). Sonic hedgehog mediates the polarizing activity of the ZPA. *Cell* **75**, 1401-1416.

Roy, S. and Gardiner, D. M. (2002). Cyclopamine induces digit loss in regenerating axolotl limbs. *J Exp Zool* **293**, 186-190.

Sagai, T., Hosoya, M., Mizushina, Y., Tamura, M. and Shiroishi, T. (2005). Elimination of a long-range cis-regulatory module causes complete loss of limb-specific Shh expression and truncation of the mouse limb. *Development* **132**, 797-803.

Sagai, T., Masuya, H., Tamura, M., Shimizu, K., Yada, Y., Wakana, S., Gondo, Y., Noda, T. and Shiroishi, T. (2004). Phylogenetic conservation of a limb-specific, cis-acting regulator of Sonic hedgehog (Shh). *Mamm Genome* **15**, 23-34.

Satoh, A., Endo, T., Abe, M., Yakushiji, N., Ohgo, S., Tamura, K. and Ide, H. (2006). Characterization of Xenopus digits and regenerated limbs of the froglet. *Dev Dyn* **235**, 3316-3326.

Suzuki, M., Hayashi, T., Inoue, T., Agata, K., Hirayama, M., Shigenobu, S., Takeuchi, T., Yamamoto, T. and Suzuki, K. T. (2018). Cas9 ribonucleoprotein complex allows direct and rapid analysis of coding and noncoding regions of target genes in Pleurodeles waltl development and regeneration. *Dev Biol* **443**, 127-136.

Suzuki, M., Satoh, A., Ide, H. and Tamura, K. (2005). Nerve-dependent and -independent events in blastema formation during Xenopus froglet limb regeneration. *Dev Biol* **286**, 361-375.

Suzuki, M., Yakushiji, N., Nakada, Y., Satoh, A., Ide, H. and Tamura, K. (2006). Limb regeneration in Xenopus laevis froglet. *ScientificWorldJournal* **6 Suppl 1**, 26-37.

Torok, M. A., Gardiner, D. M., Izpisúa-Belmonte, J. C. and Bryant, S. V. (1999). Sonic hedgehog (shh) expression in developing and regenerating axolotl limbs. *J Exp Zool* **284**, 197-206.

Tschumi, P. A. (1957). The growth of the hindlimb bud of Xenopus laevis and its dependence upon the epidermis. *J Anat* **91**, 149-173.

Wingender, E. (2008). The TRANSFAC project as an example of framework technology that supports the analysis of genomic regulation. *Brief Bioinform* **9**, 326-332.

Yakushiji, N., Suzuki, M., Satoh, A., Sagai, T., Shiroishi, T., Kobayashi, H., Sasaki, H., Ide, H. and Tamura, K. (2007). Correlation between Shh expression and DNA methylation status of the limb-specific Shh enhancer region during limb regeneration in amphibians. *Dev Biol* **312**, 171-182.

Yakushiji, N., Yokoyama, H. and Tamura, K. (2009). Repatterning in amphibian limb regeneration: A model for study of genetic and epigenetic control of organ regeneration. *Semin Cell Dev Biol* **20**, 565-574.

Yokoyama, H., Endo, T., Tamura, K., Yajima, H. and Ide, H. (1998). Multiple digit formation in Xenopus limb bud recombinants. *Dev Biol* **196**, 1-10.

Yoshida, K., Urase, K., Takahashi, J., Ishii, Y. and Yasugi, S. (1996). Mucus-associated antigen in epithelial cells of the chicken digestive tract: developmental change in expression and implications for morphogenesis-function relationships. *Dev. Growth Differ.* **38**, 185-192.

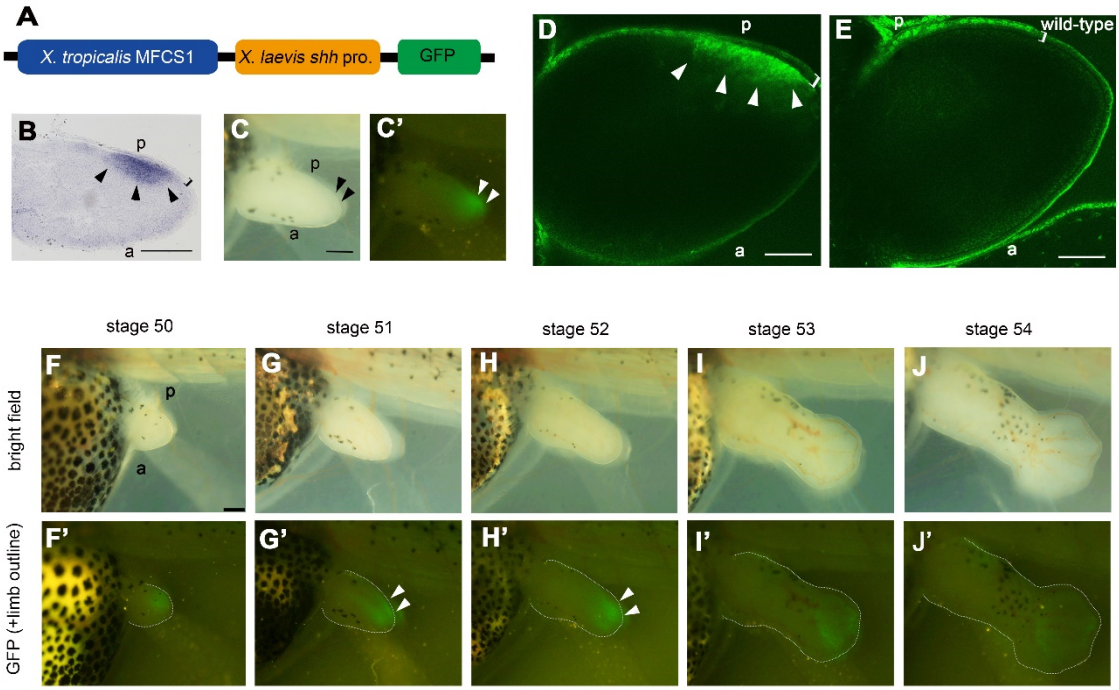

669

670 **Fig. 1. MFCS1-GFP expression coincides with *shh* expression in a developing limb**
671 **bud.** (A) Map of the MFCS1-GFP transgene. (B) *shh* expression in a limb bud at stage
672 52. (C, C') A limb bud of an MFCS1-GFP tadpole at stage 51. Bright-field (C) and
673 fluorescent (C') images. (D, E) Optical-section images by confocal microscopy
674 (approximately 60-70 μm in depth from the dorsal surface) of the right limb bud of an
675 MFCS1-GFP tadpole (D) and that of a wild-type tadpole (E) at stage 51. Bright-field (F-
676 J) and fluorescent (F'-J') images of the left limb bud of the same MFCS1-GFP tadpole.
677 Limb buds are outlined by dotted lines in the fluorescent images. All of the MFCS1-GFP
678 tadpoles shown are line 1. a, anterior: p, posterior. Arrowheads show *shh* expression (B)
679 or GFP expression (D, E, G', H') at the posterior side. Brackets indicate the epidermal
680 cell layer. Bars = 100 μm for (B, D ,E) and 200 μm for (C, C', F-J, F'-J').

681

682

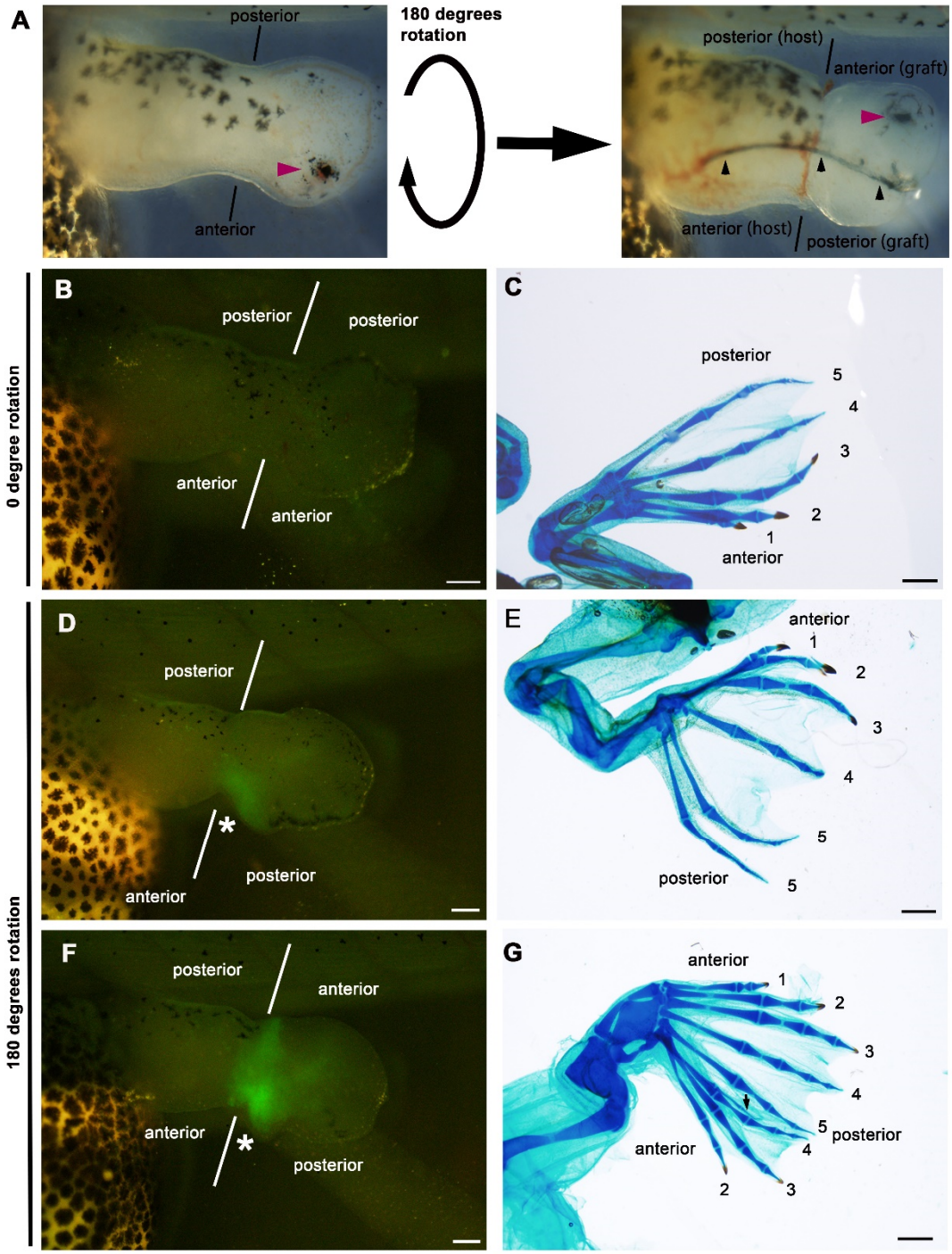

683

684 **Fig. 2. MFCS1-GFP expression precedes limb duplication along the AP axis in 180°**
685 **rotated limb buds.** (A) 180° rotation of a limb bud at stage 53. A magenta arrowhead
686 indicates an embedded Nile blue A particle. Note the inverted position of the particle
687 before (lower side) and after (upper side) grafting. Black arrowheads indicate a tungsten
688 pin. (B, C) A 0° rotated limb bud at 6 days after grafting (B) and the resultant normal limb

689 formation (C). (D-G) 180° rotated limb buds. Rotated limb buds at 6 days after grafting
690 (D,F) resulted in supernumerary limb formation (E,G). Note that the sample with brighter
691 GFP (F) resulted in more supernumerary limbs (G). All of the operated MFCS1-GFP
692 tadpoles are line 1. A pair of lines indicates the host-graft boundary. An asterisk indicates
693 ectopic GFP. An Arabic number indicates the digit identify. A black arrow shows an
694 unidentifiable digit. Bars = 200 μm for (B, D, F) and 1 mm for (C, E, F).
695

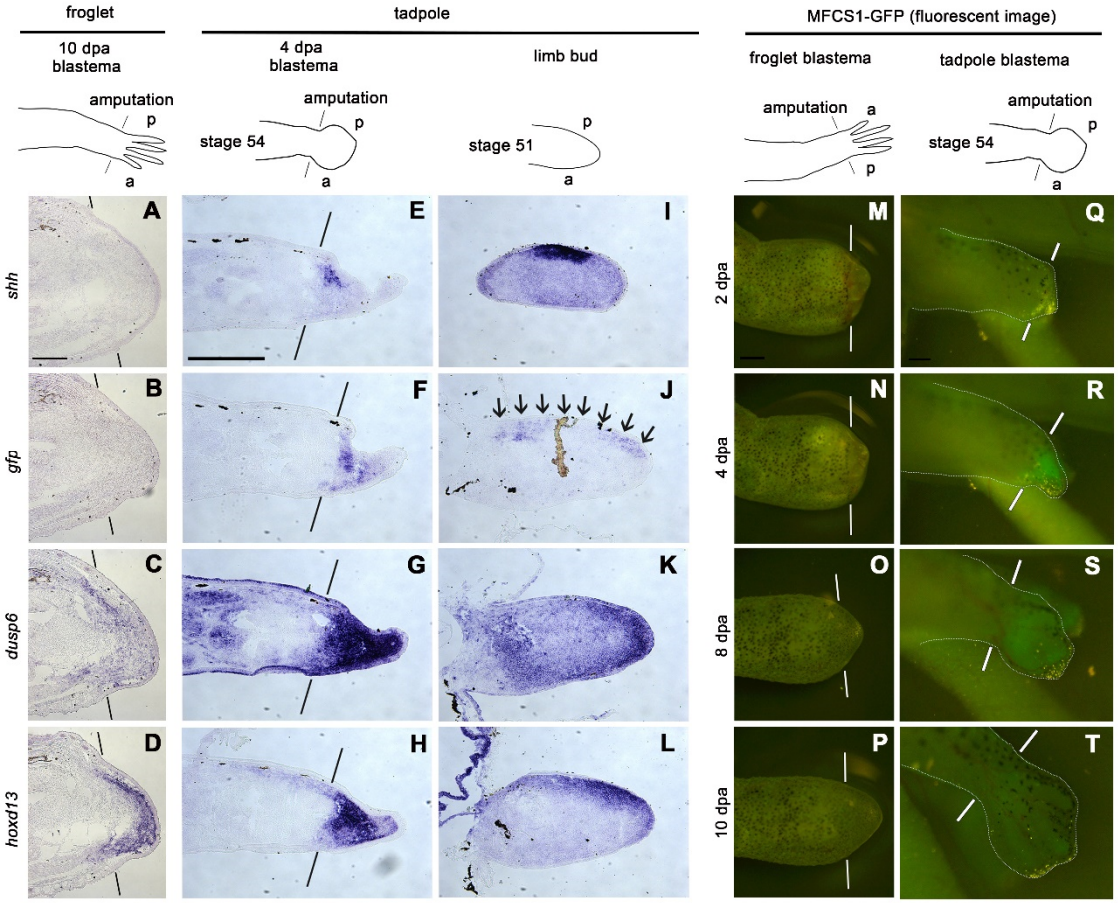

Fig. 3. Comparison of gene expression patterns and MFCS1-GFP expression pattern in a regenerating limb in a young tadpole and a froglet. (A-D) Adjacent sections of a blastema of a froglet. n=5 of 5 blastemas from a total of five froglets of line 1. (E-H) Adjacent sections of a blastema of a tadpole. (I-L) Adjacent sections of a limb bud. n=9 of 9 blastemas from a total of five tadpoles of line 1 and 6 of 6 blastemas from a total of three tadpoles of line 2, respectively. n=10 of 10 limb buds from a total of five tadpoles of line 1 and 6 of 6 from a total of three tadpoles of line 2, respectively. (M-P) A blastema of a froglet of line 1. See also Fig. S3 for details. (Q-T) A blastema of a tadpole of line 1. The blastema and the stump are outlined by a dotted line. See also Fig. S2 for details. a, anterior: p, posterior. A pair of lines indicates the amputation level. Arrows indicate *gfp* expression at the posterior side. All pictures shown in Fig. 3 are samples of line 1. Bar = 200 μm for (A-L, Q-T) and 500 μm for (M-P).

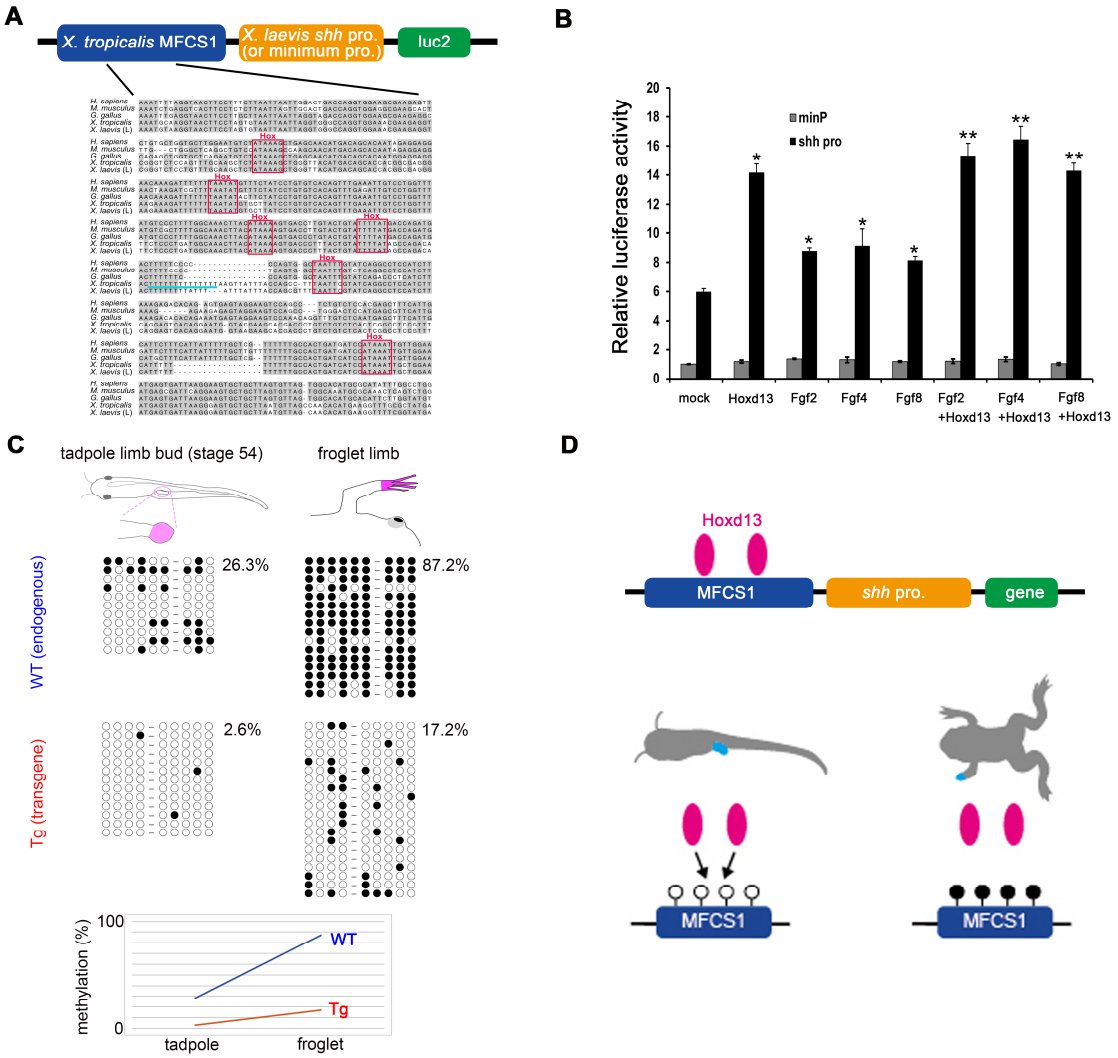

Fig. 4. Transactivation and DNA methylation of *Xenopus* MFCS1 enhancer. (A) Upper panel: Map of MFCS1-luc2 used for assays in (B). Lower panel: Alignment of MFCS1 highly conserved sequences. Nucleotides identical in more than two sequences are shaded in grey. Conserved Hox-binding motifs are boxed. A light bule line underlies the 14-thymidine repeat in *X. tropicalis* (See Materials and Methods for details.). (B) Firefly luciferase activity of MFCS1-luc2 using a minimum promoter (minP) or *shh* promoter (shh pro) was normalized to *Renilla* luciferase control activity. The mean value of mock samples by the control construct with the minimum promoter was adjusted to 1.0. Error bars, standard deviation from the mean (n=3). *Significant increase from mock ($p<0.01$). **Significant increase in Fgf2+Hoxd13, Fgf4+Hoxd13 and Fgf8+Hoxd13 from sole Fgf2, Fgf4 and Fgf8, respectively ($p<0.01$). (C) Methylation pattern of endogenous and transgene MFCS1 (line 1). Samples were obtained from the autopod (pink). Each

723 circle corresponds to a CpG site (see Fig. S6). Lower panel: Increases in average
724 methylation rate of the MFCS1 sequences after metamorphosis. (D) Model for epigenetic
725 silencing of gene expression through DNA methylation of MFCS1. Hoxd13 activates
726 hypomethylated MFCS1 and results in transcription of a gene under control of MFCS1
727 in the tadpole limb (left). However, Hoxd13 is unable to activate highly methylated
728 MFCS1 in a froglet limb and results in inactive transcription of the gene (right).
729

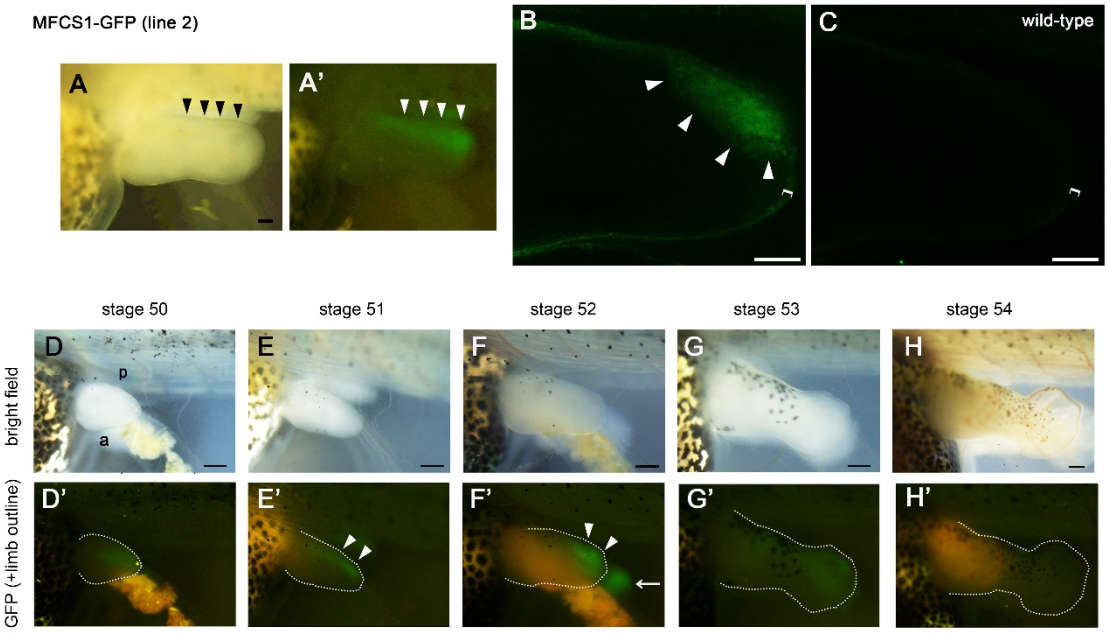

730

731 **Fig. S1. MFCS1-GFP expression pattern was recapitulated in line 2.** (A) A developing
732 limb bud of an MFCS1-GFP Tg tadpole of line 2 at stage 52. Bright-field (A) and
733 fluorescent (A') images of the same limb bud. (B, C) Optical-section images by confocal
734 microscopy (approximately 80 μm in depth from the dorsal surface) of the right limb bud
735 of an MFCS1-GFP Tg tadpole of line 2 (B) and a wild-type tadpole (C) at stage 52. GFP
736 expression was detected in the posterior side mesenchyme specifically in the MFCS1-
737 GFP Tg tadpole. Bright field (D-H) and fluorescent (D'-H') images of the limb bud of
738 the same Tg tadpole of line 2. Limb buds are outlined by dotted lines. GFP expression
739 was detected in the posterior side of limb buds at stage 51-52 and then gradually
740 diminished. a, anterior: p, posterior. Arrowheads show GFP expression (A, A', B, E', F')
741 at the posterior side of the limb buds. Brackets indicate the epidermal cell layer. A pair of
742 lines indicates the amputation level. Bars = 100 μm for (A, B, C), 200 μm for (D-H, D'-
743 H').

744

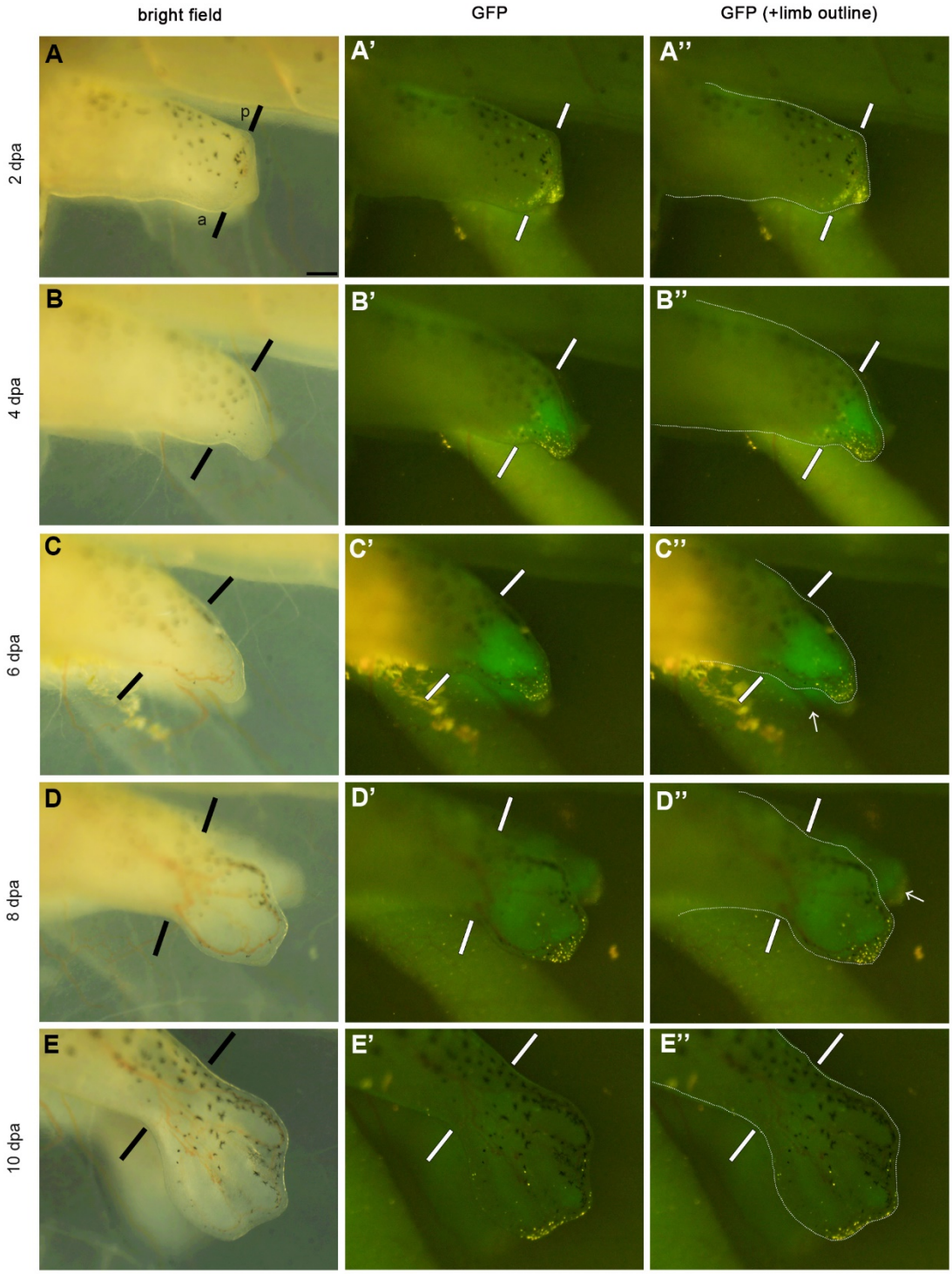

745

746 **Fig. S2. Spatio-temporal expression pattern of MFCS1-GFP in a regenerating limb**
747 **of a young tadpole.** All of the pictures are focused on a limb blastema of the same tadpole
748 (identical to Fig. 3Q-T) of line 1. Left and right limb buds were amputated at the
749 presumptive ankle level of a stage 54 tadpole. GFP fluorescence was distributed

750 throughout the regenerating limb blastema at 4 dpa and 6 dpa. (A'', B'', C'', D'', E''')
751 Limb blastemas and stumps are outlined by dotted lines. n=16 of 16 blastemas from a
752 total of ten MFCS1-GFP tadpoles of line 1 and 6 of 6 blastemas from a total of three
753 MFCS1-GFP tadpoles of line 2, respectively. A pair of lines indicates the amputation
754 level. Arrows show GFP fluorescence of the contralateral right limb blastemas. a,
755 anterior: p, posterior. Bar = 200 μm.
756

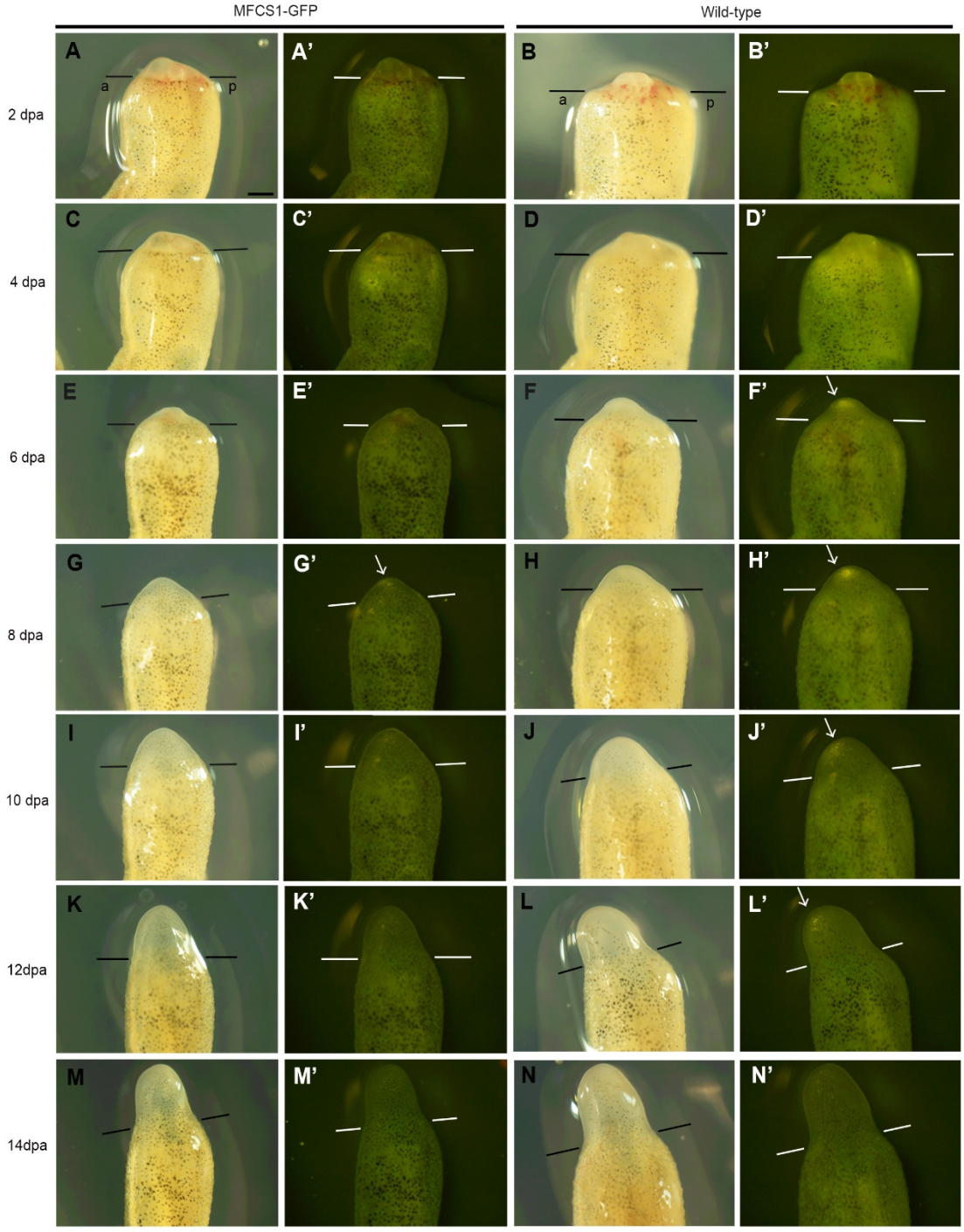

757

758 **Fig. S3. MFCS1-GFP expression is inactive in a limb blastema of a froglet.** A blastema
759 of the same froglet of line 1 (right two columns; identical to Fig. 3M-N) and a blastema
760 of the same wild-type froglet (left two columns) from 2 dpa to 14 dpa. No specific GFP
761 fluorescence was observed in the blastema of the Tg froglet at any timepoint. n=4 of 4
762 blastemas from a total of four froglets of line 1, 6 of 6 blastemas from a total of four

763 froglets of line 2 and 8 of 8 blastemas from a total of six wild-type froglets as controls,
764 respectively. A pair of lines indicates the amputation level. An arrow indicates non-
765 specific fluorescence commonly observed both in the Tg froglet and wild-type one. a,
766 anterior: p, posterior. Bar = 500 μm.
767

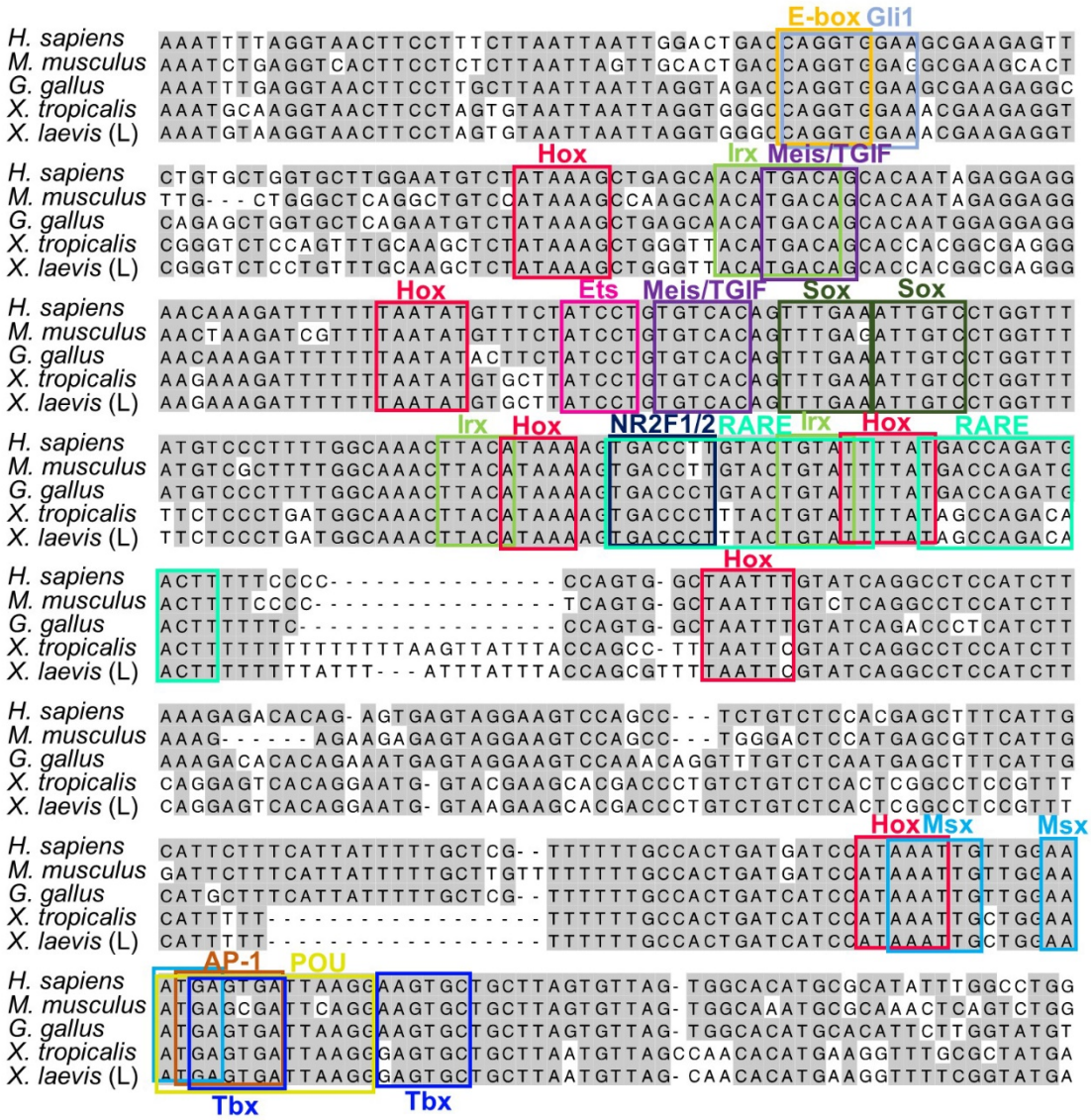

Fig. S4. Alignment of MFCS1 highly conserved sequences (identical sequences shown in Fig. 4A) from the human, mouse, chick, *X. tropicalis* and *X. laevis*. Nucleotides identical in more than two sequences are shaded in grey. Conserved transcription factor-binding motifs (Hox and other transcription factors) are boxed.

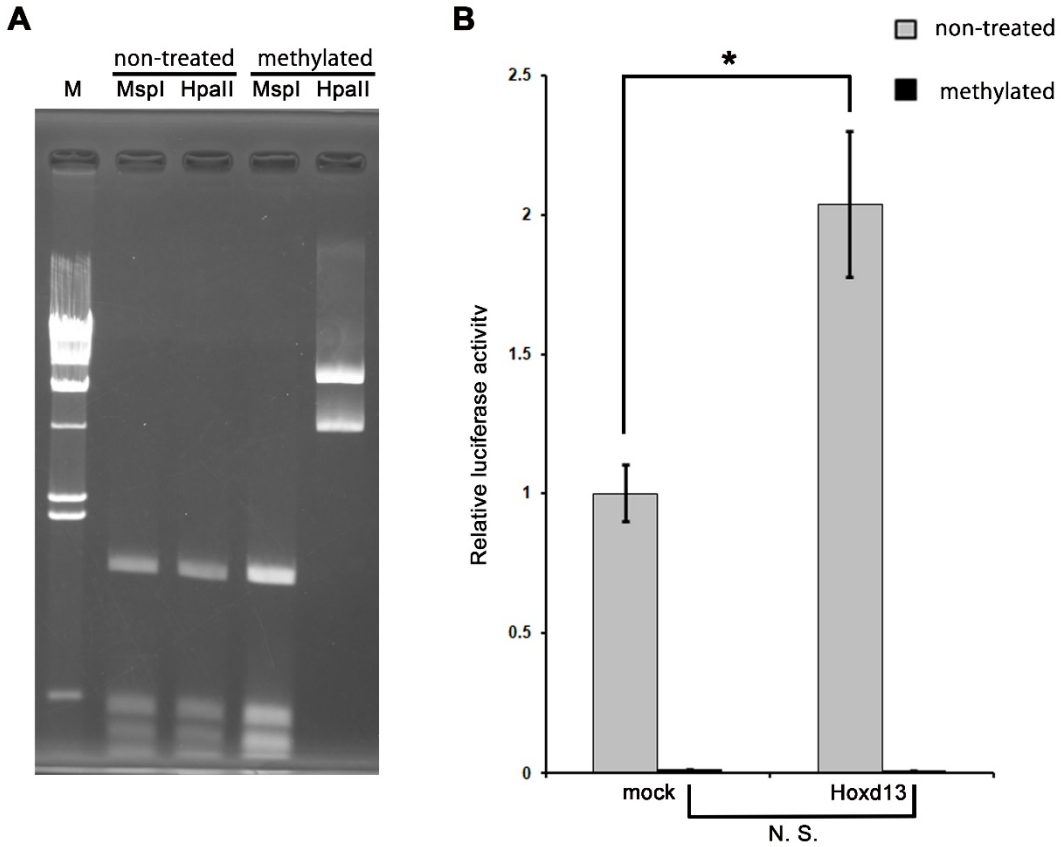

774

775 **Fig. S5. DNA methylation suppresses the response of MFCS1 to Hoxd13 *in vitro*.**
776 (A) Methylation-sensitive restriction digestion visualized by agarose gel
777 electrophoresis. Plasmid DNA of the MFCS1-*shh* promoter-*luc2* reporter was treated
778 with CpG methyltransferase (M. SssI, NEB) according to the manufacturer's protocol.
779 Methylation efficiency of the plasmid DNA was evaluated by digestion with
780 methylation-sensitive (HpaII) and -insensitive (MspI) restriction enzymes. The CpG
781 methylation prohibited the digestion of the plasmid DNA specifically with HpaII. M,
782 l/HindIII marker. (B) Luciferase activity in NIH3T3 cells transfected with the
783 methylated or non-treated MFCS1-luc2 reporter constructs and the *Hoxd13* expression
784 construct. The mean value of luciferase activity in cells transfected with the non-treated
785 reporter and mock expression constructs was set to 1.0. Error bars: standard deviation
786 from the mean (n=3). While a significant increase of *Hoxd13*-induced luciferase activity
787 was observed in cells transfected with the unmethylated reporter construct (*$p<0.01$),
788 being consistent with Fig. 4B, there was no significant increase in cells transfected with
789 the methylated reporter construct despite *Hoxd13* expression. N. S., not significant.

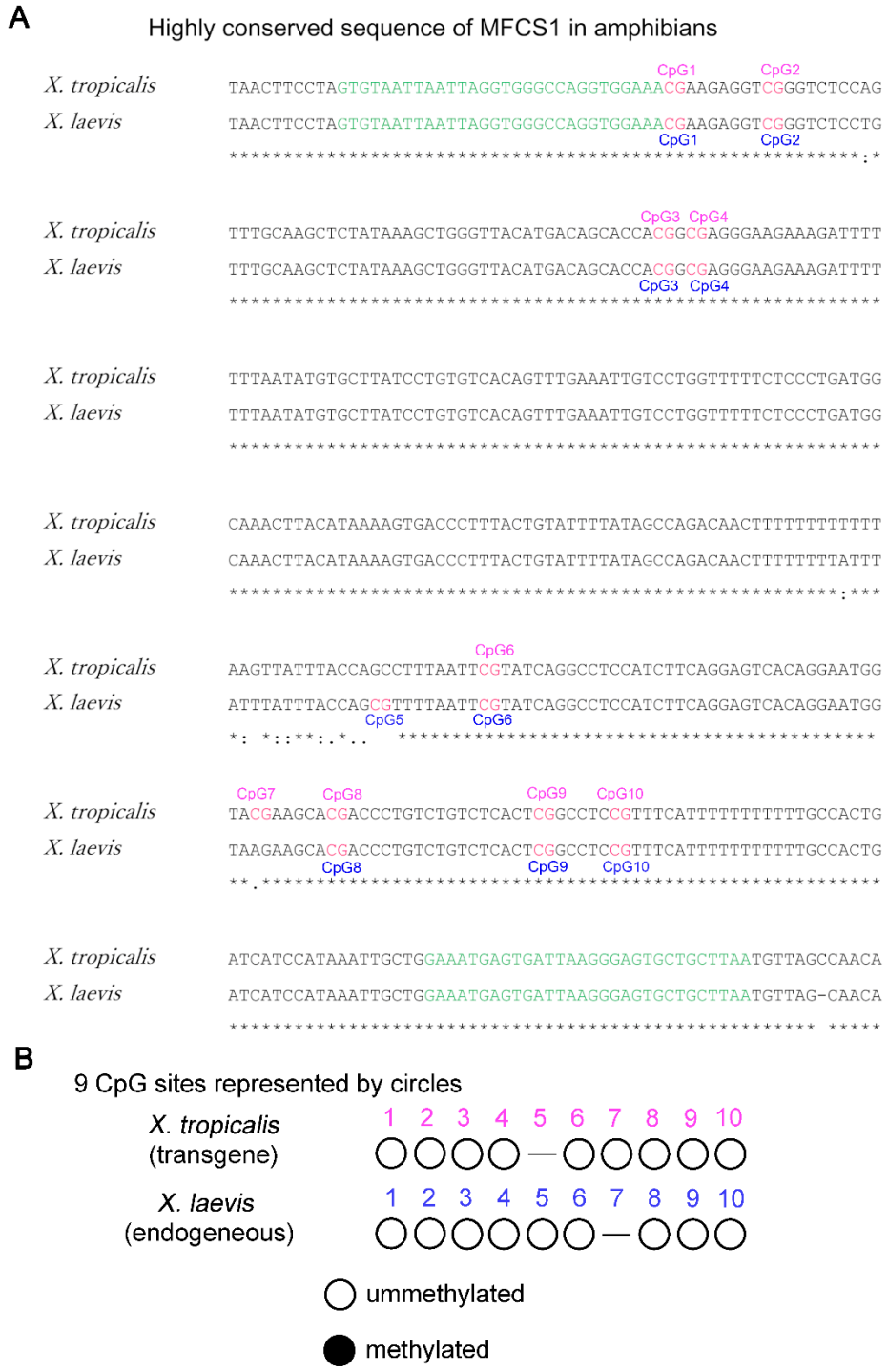

Fig. S6. *X. tropicalis* and *X. laevis* have 9 CpG sites in the highly conserved sequence of MFCS1. Alignment of MFCS1 highly conserved sequences between *X. tropicalis* and *X. laevis*. Green letters correspond to MFCS1_BS_Fw and MFCS1_BS_Rv primers for bisulfite sequencing (see also Table S3). Open and black circles represent unmethylated and methylated CpG sites, respectively.

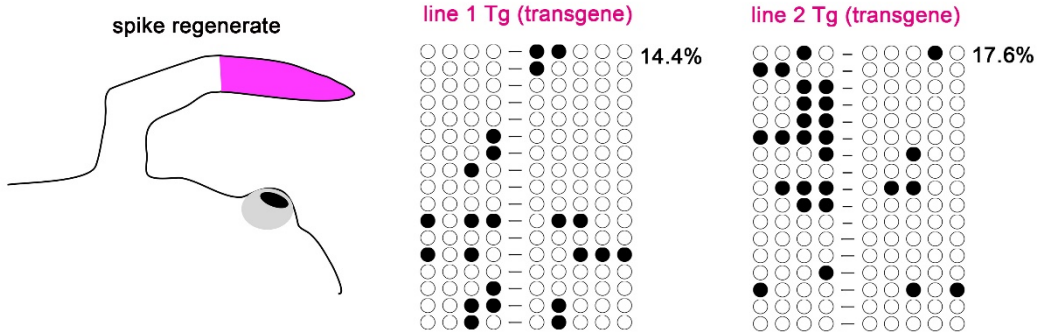

Fig. S7. Methylation pattern of MFCS1 in a spike regenerate after limb regeneration of a froglet. After limb blastemas of froglets completed spike regeneration, regenerate samples (pink) were obtained from line 1 and line 2 Tg frogs.

Table S1. Rate of germline transmission and activity of MFCS1-GFP

G0	N1	N2
	GFP+/ total	GFP+/ total
line 1	195/368 (53%)	70/172 (41%)
line 2	79/180 (44%)	not applicable

Table S2. Supernumerary limb formation and ectopic GFP in rotated limb buds

180° rotated limb buds

Sample	No. of original digits	No. of supernumerary digits	No. of digits (total)	Is there ectopic GFP?	Figure
1	5	2	7	Yes	-
2	5	2	7	Yes	-
3	5	2	7	Yes	-
4	5	2	7	Yes	-
5	5	4	9	Yes	Fig. 2F, G
6	5	2	7	Yes	-
7	5	1	6	Yes	Fig. 2D, E
8	5	0	5	No	-
9	5	0	5	No	-
10	5	0	5	No	-
11	5	2	7	Yes	-

0° rotated limb buds (controls)

Sample	No. of original digits	No. of supernumerary digits	No. of digits (total)	Is there ectopic GFP?	Figure
1	5	0	5	No	Fig. 2B, C
2	5	0	5	No	-
3	5	0	5	No	-
4	5	0	5	No	-
5	5	0	5	No	-
6	5	0	5	No	-
7	5	0	5	No	-
8	5	0	5	No	-
9	5	0	5	No	-
10	5	0	5	No	-
11	5	5	10	Yes	-
12	5	3	8	Yes	-

Table S3. Primers for genomic- and RT-PCR

name	Sequence (5’ -> 3’)	note
xtMFCS1-Fw	ACTGTAACCAGTGAAAATCATCAGTCATGAATATC	transgene
xtMFCS1-Rv	TGGCCTAGTTCATAGACATTAATTATTTTTCTATGGG	transgene
xtM1-Acc65I-Fw	ttggtaccTTCAAATGATGGATTTTCATATTATAA	Luc reporter
xtM1-XhoI-Rv	ggctcgaGACCATGAAGGCACCCTAATACT	Luc reporter
xlpS-XhoI-Fw	ggctcgAGTGACACCGTGGAAGCCTTTATTATC	Luc reporter
xlpS-NcoI-Rv	ggccatggtGTCCGAGCGAAGCCAATTACATCA	Luc reporter
Fgf2_cds_F1	GCCATGGCTGCCAGCGGCATCACC	Gene Expression
Fgf2_cds_R1	TCAGCTCTTAGCAGACATTGGAAG	Gene Expression
Fgf4_cds_F1	CCGGGATGGCGAAACGCGGGCCGA	Gene Expression
Fgf4_cds_R1	TCACAGTCTAGGAAGGAAGTGGGT	Gene Expression
Fgf8_cds_F1	GACCCCGCTCGGGCTCTCAGTGCT	Gene Expression
Fgf8_cds_R1	CTATCGGGGCTCCGGGGCCCAAGT	Gene Expression
Hoxd13-F	ATGAGCCGCTCGGGGACTTG	Gene Expression
Hoxd13-R	TCAGGAGACAGTGTCTTTGA	Gene Expression
MFCS1_BS_Fw	GTGTAATTAATTAGGTGGGyyAGGTGGAAA	Bisulfite sequencing
MFCS1_BS_Rv	TTAArCArCACTCCCTTAATCACTCATTTC	Bisulfite sequencing
M13F-pUC	GTTTTCCCAGTCACGAC	Bisulfite sequencing
M13R-pUC	CAGGAAACAGCTATGAC	Bisulfite sequencing